https://doi.org/10.30799/jnst.256.19050404 J. Nanosci. Tech. - Volume 5 Issue 4 (2019) 758–760

ISSN: 2455-0191

Share Your Innovations through JACS Directory

Journal of Nanoscience and Technology

Visit Journal at http://www.jacsdirectory.com/jnst

Investigation of Structural, Electrical and Thermal Characteristics of $NdFeO_3$ Ceramic

Vikash Kumar Jha*, M. Roy

Department of Physics, Mohanlal Sukhadia University, Udaipur-313001, Rajasthan, India.

ARTICLEDETAILS

Article history:
Received 21 May 2019
Accepted 07 June 2019
Available online 12 June 2019

Keywords:
Perovskites
Solid-State Reaction
Rietveld Refinement

ABSTRACT

The synthesis of single phase polycrystalline ceramic sample of $NdFeO_3$ by high temperature solid state reaction technique using high purity oxides has been reported. The structural parameters were investigated by Rietveld refinement program. The prepared ceramics show orthorhombic structure with space group Pnma. The frequency and temperature dependent dielectric constant, dielectric loss and ac conductivity of the compound have been studied. The dc conductivity has also been measured and its activation energies were calculated using Arrhenius relation. The calculated heat capacity (ΔC_p) and enthalpy change (ΔH) of the compound are 0.068 J/gK and 2.3664 J/g respectively.

1. Introduction

Rare earth based orthoferrite ceramics attract great attention due to spin reorientation, phase transition, high domain wall velocity, weak ferro-magnetic behavior with rectangular hysteresis loop and smaller magnetic field due to presence of rare earth elements and iron ions [1-7]. Due to these properties, these orthoferrites have been extensively studied for various technological applications such as ultrafast photo magnetic recording, non-thermal spin dynamics, laser induced ultrafast spin reorientation, photo catalysis, solid oxide fuel cells, vehicle catalytic converters, inertia driven spin switching, ambient multiferroics, magnetic field sensors, gas sensors for CO, H_2S and magneto-optical data storage devices [8-12]. $NdFeO_3$ has been synthesized by different methods such as sol-gel method, precipitation, floating zone, flux-melting, solid state reaction etc. $NdFeO_3$ (NFO), exhibits an orthorhombic distorted perovskite structure belonging to the space group Pbnm D_{2h}^{16} [13,14]. There is no any detailed report available on structural, electrical and thermal properties of NFO ceramic so the present paper is an effort to understand the mechanism of this compound which will be useful for researchers to implement the physical characteristics of $NdFeO_3$ in different technological applications.

2. Experimental Methods

The polycrystalline ceramic sample of $NdFeO_3$ has been prepared by solid state reaction technique. The constituent oxides Nd_2O_3 and Fe_2O_3 (99.9% pure, Hi-media) were grinded together in a mortar and pestle under liquid medium [$(CH_3)_2CO$] and calcined at different temperatures (1073 K – 1498 K) continuously for 6 to18 hours. Pellets were made with pressures 4 tons/cm^2 in a hydraulic press. This pellet was sintered at 1513 K for 2 hours. The formation of the compound was checked by X-ray diffraction technique using Rigaku Mini Flex ULTIMA-IV X-ray Diffractometer (XRD) with slow scan (2° / minute) in a wide range of 2θ (20° to 90°). The lattice parameters of obtained XRD pattern were obtained from Rietveld refinement method. HIOKI 3532-50 LCR Hi-meter has been implement for the measurement of dielectric constant (ε') and dielectric loss (tan δ) as a function of frequency (1 kHz - 5 MHz) and temperature (RT - 723 K).

Also, the ac-conductivity of compound has been calculated from temperature dependent dielectric loss curve. The dc conductivity measurement was carried out on laboratory-made set up using two probe method from RT to 543 K and the activation energies of the compound were calculated by Arrhenius relation, $\sigma = \sigma_0 \exp\left(\frac{-E_a}{kT}\right)$. The heat flow (mW) and weight loss (mg) of the compound were carried out under wide temperature range (RT to 1173 K) with heating rate of 10 K/minute using Perkin Elmer DTA/TGA thermal analyzer (STA- 6000) in the inert (N_2) atmosphere

3. Results and Discussion

3.1 Structural Analysis

The X-ray diffraction pattern was analyzed by FullProf program of Rietveld refinement method. The observed and calculated patterns are well matching with each other. Fig. 1 shows the refined XRD pattern with space group Pnma in orthorhombic crystal structure of the compound. The refined cell parameters are a = 5.5846 Å, b = 7.7607 Å, and c = 5.4506 Å. The crystallographic atomic positions of neodymium (Nd), iron (Fe) and oxygen (O) atoms along with the coordinates of $NdFeO_3$ are shown in Table 1. Also, the other refined structural parameters obtained from the Rietveld analysis are also shown in Table 1. The observed and calculated interplanar spacing's (d-values) have shown good agreement between them, which is tabulated in Table 2.

The crystallite size (D) of the compound was calculated using the Scherer formula, D = kλ/βcosθ [15] which is 1.57 nm. The dislocation density (δ) of the compound was calculated using the Williamson–Smallman relation δ = 1 / D^2 and the calculated value of δ is 0.000551 (nm)$^{-2}$. The strain (ε) of the compound has been calculated using the equation ε = β / 4tanθ and the calculated value of strain is 0.070093. Also, the number of crystallites per unit area (N) of the compound has been calculated using the relation N = t/D^3, where t is the thickness of the sample and the calculated value of N is 725.728 (nm)$^{-2}$.

Table 1 Crystallographic atomic position and structural parameters obtained from Rietveld analysis

Crystallographic atomic position				Structural parameters			
Atom	X	Y	Z	Unit cell volume	236.4 (Å)^3	R_p	2.73
Nd	0.548	0.25	0.510	Density	6.98 (g/cm^3)	R_{wp}	3.56
Fe	0.489	0.00	0.000	Number of Reflections	107	R_e	4.26
01	-0.019	0.25	0.398	R_{Bragg}	10.9	χ^2	0.7
02	0.303	0.041	0.717	R_f	16.3	GOF	0.83

*Corresponding Author:vkjha1988@yahoo.com(Vikash Kumar Jha)

https://doi.org/10.30799/jnst.256.19050404

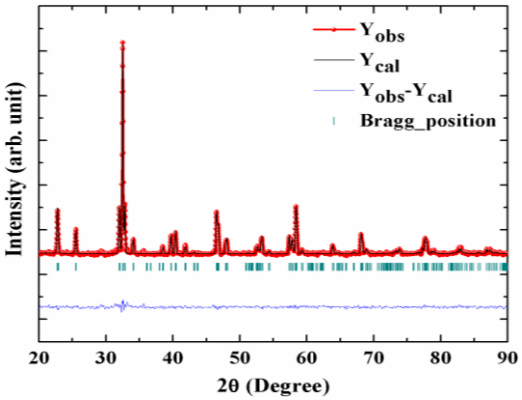

Fig. 1 Rietveld refinement profile of $NdFeO_3$

Table 2 Obtained d- values from XRD pattern of $NdFeO_3$

2θ (degree)	*h k l*	d-obs. (Å)	d-cal. (Å)
22.735	1 0 1	3.9013	3.9001
25.533	1 1 1	3.4858	3.4845
32.019	2 0 0	2.7928	2.7929
32.514	1 2 1	2.7514	2.7503
32.832	0 0 2	2.7256	2.7250
34.088	2 1 0	2.6279	2.6295
38.305	1 3 0	2.3477	2.3472
39.728	2 2 0	2.2669	2.2660
40.404	0 2 2	2.2305	2.2304
41.859	1 3 1	2.1563	2.1565
46.517	2 0 2	1.9506	1.9505
48.053	2 1 2	1.8918	1.8972
52.633	1 4 1	1.7375	1.7365
53.268	3 1 1	1.7182	1.7166
57.385	3 2 1	1.6043	1.6038
57.808	2 4 0	1.5936	1.5926
58.413	1 2 3	1.5785	1.5783
63.863	3 3 1	1.4563	1.4561
68.175	4 1 0	1.3738	1.3753
73.823	3 1 3	1.2825	1.2809
77.700	1 6 1	1.2279	1.2258
83.047	3 3 3	1.1619	1.1598
87.366	0 4 4	1.1152	1.1141

3.2 Electrical Analysis

Dielectric constant (ε') and Dielectric loss (tan δ) as a function of frequency (100 Hz to 5 MHz) have been measured at room temperature and is shown in Fig. 2. From Fig. 2, it is observed that dielectric constant is decreasing with increase in frequency. The inefficacy of electric dipoles which is produced by applied electric field supports the decreasing trend of ε' at high frequency region. Due to the presence of all types of polarizations which align themselves in one direction with the applied electric field, ε' shows high apparent values at low frequency region and small apparent values in high frequency region and it is explained by dipole relaxation phenomenon in the ceramics. However, a reverse trend was obtained for the tan δ, which is the imaginary part of the dielectric constant. Dielectric loss (tan δ) shows increasing trend with increase of frequency due to higher conductivity which leads the leakage current phenomena in the ceramics. Both ε' and tan δ shows small dispersion (in the insets of the Fig. 2) with increase in frequency (From 1 MHz to 1.6 MHz) which support the Maxwell-Wagner type interfacial polarization and also the Koop's theory [16].

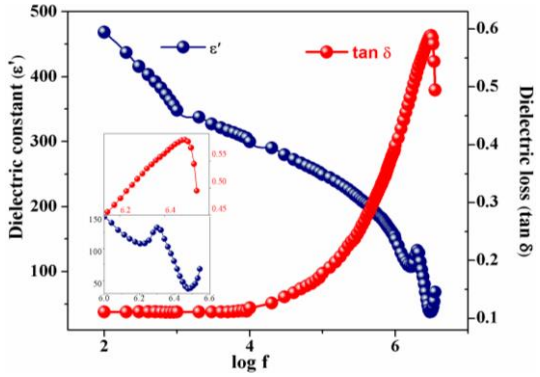

Fig. 2 ε' and tan δ vs. frequency curve

https://doi.org/10.30799/jnst.256.19050404

Dielectric constant (ε') as a function of temperature (K) has been measured over 10 kHz, 100 kHz, and 1 MHz frequencies and is shown in Fig. 3. At high temperature, the ε' shows high magnitude in all measured frequencies which supports the strong temperature dependent nature for dielectric constant of the sample. Dielectric constant (ε') shows increasing trend with increase of temperature but no any phase transition has been observed up to the measured temperature region. With increase in temperature, the effect of charge polarization is enhancing hence the permittivity rise to apparent values which shows the electrical insulation characteristic of the sample. The increasing trend of ε' with temperature in all measured frequencies support the dipoles mechanism in the pellet. However, the ε' show a sluggish dip in between 10 kHz to 1 MHz frequencies due to smaller crystallite size of the compound, which is the characteristic of a good dielectric material. Dielectric loss (tan δ) as a function of temperature over the measured frequencies is shown in Fig. 4. From Fig. 4, we see the decreasing trend in magnitude of dielectric loss with increase in frequency. Also, the tan δ increases with increase of temperature in all measured frequencies. This increment in tan δ with increase of temperature supports the leakage current phenomenon. Hence, we can say that the prepared material behaves like a conductor in high temperature zone.

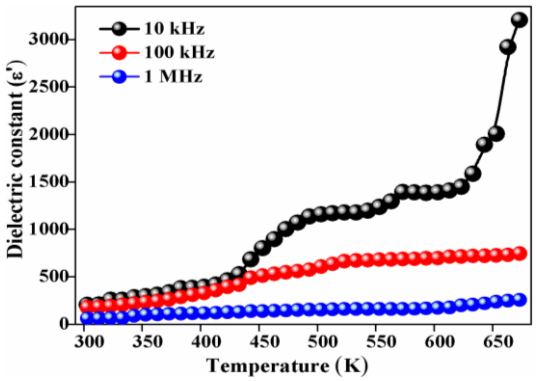

Fig. 3 ε' vs. temperature curve

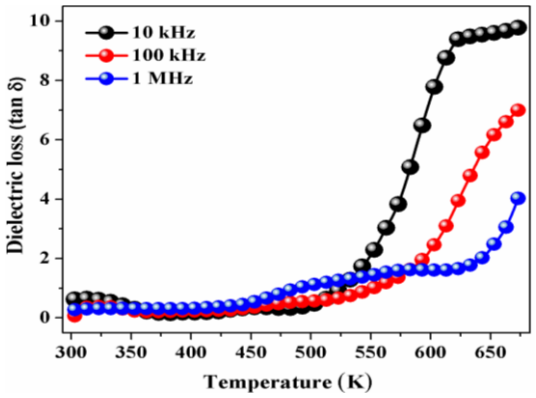

Fig. 4 tan δ vs. temperature curve

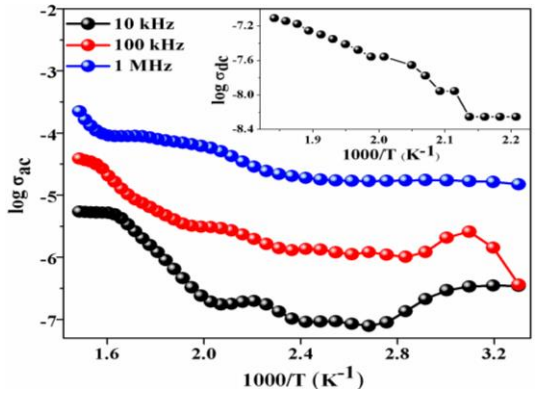

Fig. 5 log σ_{ac} vs. 10^3/T curve (log σ_{dc} vs. 10^3/T curve is in inset)

The ac-conductivity measured at different frequencies (10 kHz, 100 kHz and 1 MHz) show increasing trend with increase of temperature which is shown in Fig. 5. Due to oxygen ion vacancy, the magnitude of log σ_{ac} increases with increase in frequency (from 10 kHz to 1 MHz). The dc-conductivity of the sample is shown in the inset of Fig. 5. The conductivity (log σ_{dc}) increases with increase in temperature under dc-field. This

increment in conductivity with increase in temperature occurs due to impurities, interstitials, defects etc. takes place either through band mechanism or through hopping of the charge carriers among impurity centers. Also, the increase in conductivity is a consequence of thermally activated process which can be described by the Arrhenius relation. The calculated activation energies (E_a) are 2.69 eV and 1.73 eV for the temperature ranges (473 K to 498 K) and (503 K to 543 K) respectively.

3.3 Thermal Studies

The heat flow vs. temperature curve in the heating and cooling cycles for neodymium ferrite is shown in Fig. 6. The endothermic sluggish peak around 1103 K in heating cycle has been observed. This sluggish peak around 1103 K is the ferroelectric transition temperature/Curie temperature (T_C) of the sample and the magnified view near Curie temperature is shown in the Fig. 6. There are no any major/sluggish peaks have been observed in cooling cycle. The calculated values of change in heat flow (ΔCp) and change in enthalpy (ΔH) are 0.068 J/gK and 2.3664 J/g respectively. Also, weight vs. temperature curve is shown in the inset of Fig. 6. The calculated value of weight loss with increase in temperature is 0.157 mg. This achieved value (0.157 mg) is 1.01 % for the initial weight of stoichiometric amount of $NdFeO_3$. This small weight loss indicates the thermal stability of the compound.

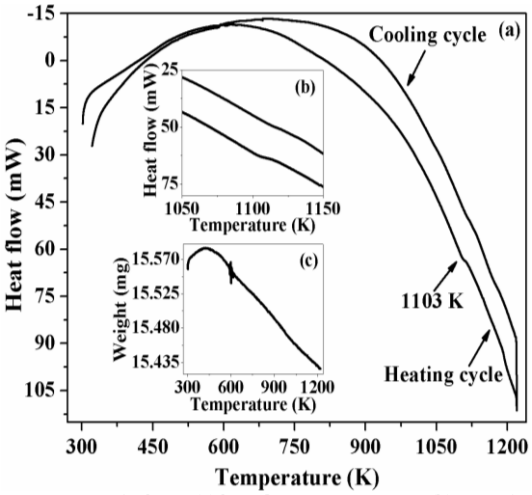

Fig. 6 DTA-TGA curve of $NdFeO_3$ (a) heat flow vs. temperature (b) magnified view of heat flow near T_C (c) weight loss vs. temperature

4. Conclusion

The polycrystalline $NdFeO_3$ ceramic has been prepared by conventional high temperature solid state reaction method. The formation of the compound exists in Pnma space group which has been confirmed by X-ray diffraction analysis and its lattice parameters were calculated using Rietveld refinement method. The high magnitude of dielectric constant at room temperature supports the dielectric relaxation phenomenon. The dielectric constant as well as dielectric loss studies support the Maxwell - Wagner type interfacial polarization. The increment in dielectric constant with increase in temperature supports the probability of electric dipoles occurrence in the sample which is the characteristic of electrical insulation. The dielectric loss shows decreasing trend with increase in frequency. Also, with increase in temperature this dielectric loss is increasing in the all measured frequencies. The activation energies (2.69 eV and 1.73 eV) were calculated in two temperature ranges (473 K to 498 K and 503 K to 543 K). The thermal analysis measurement confirms that this compound is thermally stable due to very low weight loss (1.015% of the initial weight). Hence, this detailed analysis of structural, electrical and thermal characteristics for $NdFeO_3$ ceramic will be useful for practical applications.

Acknowledgement

Authors are thankful to Dr. N. Lakshmi for her help in XRD measurement. VKJ is gratefully acknowledge the UGC-BSR fellowship.

References

[1] W. Sławiński, R. Przeniosło, I. Sosnowska, E. Suard, Spin reorientation and structural changes in $NdFeO_3$, J. Phys. Condens. Matter. 17 (2005) 4605-4614.
[2] R.L. White, Review of recent work on the magnetic and spectroscopic properties of the rare-earth orthoferrites, J. Appl. Phys. 40 (1969) 1061-1069.
[3] T. Yamaguchi, Theory of spin reorientation in rare-earth orthochromites and orthoferrites, J. Phys. Chem. Solids 35 (1974) 479-500.
[4] H. Pinto, H. Shaked, Long wavelength neutron diffraction study of the magnetic structures of $PrFeO_3$ and $NdFeO_3$, Solid State Commun. 10 (1972) 663-665.
[5] I. Sosnowsk, E. Steichelea, A. Hewatc, Reorientation phase transition in $NdFeO_3$, Physica B+C 136 (1986) 394-396.
[6] J. Bartolome, E. Palacois, M.D. Kuzmin, E.F. Bartolom, I. Sosnowska, et al., Single-crystal neutron diffraction study of Nd magnetic ordering in at low temperature, Phys. Rev. B. 55 (1997) 11432-11441.
[7] M.K. Singh, H.M. Jang, H.C. Gupta, R.S. Katiyar, Polarized Raman scattering and lattice eigenmodes of antiferromagnetic $NdFeO_3$, J. Raman Spectros. 39 (2008) 842-848.
[8] J.A.D. Jong, A.V. Kimel, R.V. Pisarev, A. Kirilyuk, T. Rasing, Laser-induced ultrafast spin dynamics in $ErFeO_3$, Phys. Rev. B 84 (2011) 104421:1-8.
[9] A.V. Kimel, A. Kirilyuk, A. Tsvetkov, R.V. Pisarev, T. Rasing, Laser-induced ultrafast spin reorientation in the antiferromagnet $TmFeO_3$, Nature 429 (2004) 850-853.
[10] A.V. Kimel, A. Kirilyuk, P.A. Usachev, R.V. Pisarev, A.M. Balbashov, T. Rasing, Ultrafast non-thermal control of magnetization by instantaneous photomagnetic pulses, Nature 435 (2005) 655-657.
[11] A.V. Kimel, B.A. Ivanov, R.V. Pisarev, P.A. Usachev, A. Kirilyuk, T. Rasing, Inertia-driven spin switching in antiferromagnets, Nat. Phys. 5 (2009) 727-731.
[12] J.H. Lee, Y.K. Jeong, J.H. Park, M.A. Oak, H.M. Jang, et al., Spin-canting-induced improper ferroelectricity and spontaneous magnetization reversal in $SmFeO_3$, Phys. Rev. Lett. 107 (2011) 117201:1-4.
[13] H. Taguchi, Relationship between crystal structure and electrical properties of Nd $(Cr_{1-x}Fe_x)$ O_3, J. Solid State Chem. 131 (1997) 108-114.
[14] A.G. Gavriliuk, I.A. Troyan, R. Boehler, M.I. Eremets, I.S. Lyubutin, N.R. Serebryanaya, Electronic and structural transitions in $NdFeO_3$ orthoferrite under high pressures, JETP Lett. 77 (2003) 619–624.
[15] A. Khorsand Zak, W.H. Abd. Majid, M.E. Abrishami, R. Yousefi, X-ray analysis of Zno nanoparticles by Williamson-Hall and size-strain plot methods, Solid State Sci. 13 (2011) 251-256.
[16] H.C. Madhusudhana, S.N. Shobhadevi, B.M. Nagabhushana, R. Hari Krishna, M.V. Murugendrappa, H. Nagabhushana, Structural and dielectric investigations of cerium stabilized zirconia ($Zr_{1-x}Ce_xO_2$, x = 0-0.05) nanocrystals blended by wet chemical method, J. Nanosci. Technol. 5(2) (2019) 649-654.

https://doi.org/10.30799/jnst.256.19050404

Cite this Article as: Vikash Kumar Jha, M. Roy, Investigation of structural, electrical and thermal characteristics of $NdFeO_3$ ceramic, J. Nanosci. Tech. 5(4) (2019) 758–760.